Pergamon

Geochimica et Cosmochimica Acta, Vol. 64, No. 24, pp. 4165–4178, 2000

0016-7037/00 $20.00 + .00

PII S0016-7037(00)00495-6

Authigenic molybdenum formation in marine sediments: A link to pore water sulfide in the Santa Barbara Basin

YAN ZHENG,[1,*2,3] ROBERT F. ANDERSON,[1,2] ALEXANDER VAN GEEN,[1] and JAMES KUWABARA[4]

[1]Lamont-Doherty Earth Observatory, Columbia University, Palisades, NY 10964, USA
[2]Department of Earth and Environmental Sciences, Columbia University, Palisades, NY 10964, USA
[3]Queens College, City University of New York, Flushing, NY 11367, USA
[4]U. S. Geological Survey, Water Resources Division, Menlo Park, CA 94025, USA

(*Received* 29 *October*, 1999; *accepted in revised form July* 7, 2000)

Abstract—Pore water and sediment Mo concentrations were measured in a suite of multicores collected at four sites along the northeastern flank of the Santa Barbara Basin to examine the connection between authigenic Mo formation and pore water sulfide concentration. Only at the deepest site (580 m), where pore water sulfide concentrations rise to >0.1 μM right below the sediment water interface, was there active authigenic Mo formation. At shallower sites (550, 430, and 340 m), where pore water sulfide concentrations were consistently <0.05 μM, Mo precipitation was not occurring at the time of sampling. A sulfide concentration of ~ 0.1 μM appears to be a threshold for the onset of Mo-Fe-S co-precipitation. A second threshold sulfide concentration of ~ 100 μM is required for Mo precipitation without Fe, possibly as Mo-S or as particle-bound Mo.

Mass budgets for Mo were constructed by combining pore water and sediment results for Mo with analyses of sediment trap material from Santa Barbara Basin as well as sediment accumulation rates derived from ^{210}Pb. The calculations show that most of the authigenic Mo in the sediment at the deepest site is supplied by diffusion from overlying bottom waters. There is, however, a non-lithogenic particulate Mo associated with sinking particles that contributes $\leq 15\%$ to the total authigenic Mo accumulation. Analysis of sediment trap samples and supernant brine solutions indicates the presence of non-lithogenic particulate Mo, a large fraction of which is easily remobilized and, perhaps, associated with Mn-oxides.

Our observations show that even with the very high flux of organic carbon reaching the sediment of Santa Barbara Basin, active formation of sedimentary authigenic Mo requires a bottom water oxygen concentration below 3 μM. However, small but measurable rates of authigenic Mo accumulation were observed at sites where bottom water oxygen ranged between 5 and 23 μM, indicating that the formation of authigenic Mo occurred in the recent past, but not at the time of sampling. *Copyright © 2000 Elsevier Science Ltd*

1. INTRODUCTION

The marine geochemistry of Mo is characterized by its removal in H_2S-containing anoxic basins and its association with Mn-oxides under more oxygenated waters. Mo concentrations (20 to 160 μg/g) well above the crustal background levels (1 to 2 μg/g) have been observed in many anoxic basin sediments, including the Black Sea, Cariaco Trench, Framvaren Fjord and Saanich Inlet (Jacobs et al., 1987; Francois, 1988; Emerson and Huested, 1991; Ravizza et al., 1991; Crusius et al., 1996). Corresponding to the enrichment of Mo in these anoxic basin sediments, Mo depletion has been observed in the water column, indicating removal of Mo in these environment (Berrang and Grill, 1974; Emerson and Huested, 1991). Pore water Mo depletion has also been found in sediments from Santa Monica Basin (<5 μM O_2) and Chesapeake Bay (seasonally anoxic), suggesting diffusive loss of Mo into sulfide-containing anoxic sediments (Shaw et al., 1990; Colodner, 1991; Colodner et al., 1995) .

Molybdenum is also known to be related to the diagenetic cycling of Mn-oxides. Molybdenum is significantly enriched in ferromanganese nodules (Calvert and Price, 1977). Molybdenum associated with Mn-oxides is released to pore water when Mn-oxides undergo reduction, and is re-precipitated with Mn-oxides near the sediment-water interface in marine sediment (Bertine and Turekian, 1973; Brumsack and Gieskes, 1983; Malcolm, 1985; Shimmield and Price, 1986; Shaw et al., 1990; Emerson and Huested, 1991; Crusius et al., 1996). For example, in sediments underlying oxic bottom waters (Brumsack and Gieskes, 1983; Shimmield and Price, 1986) as well as the Santa Cruz Basin (<10 μM O_2) (Shaw et al., 1990), one finds Mo recycled with Mn displaying a constant Mo/Mn weight ratio of ~ 0.002.

Because anoxic basin sediments have invariably displayed enrichment of sediment Mo (20 to 160 μg/g) over crustal background, sedimentary Mo can be potentially used as a proxy of paleo-anoxia. Distinct concentration maxima in Mo up to 50 μg/g in early Quaternary sediment from the Japan Sea (Piper and Isaacs, 1996), and Mo concentration as high as 150 μg/g in sediment from the Cariaco Basin during the past 15 kyr (Dean et al., 1999), are interpreted to indicate sulfate reducing conditions of the bottom water. The pattern of enrichment of Mo and other redox sensitive metals in a sediment core located in the oxygen minimum zone (OMZ) off the Mexican Margin at $\sim 23°$N in the northeast Pacific was interpreted as reflecting a change in the intensity of the OMZ with glacial cycles (Nameroff, 1996). Lack of Mo enrichment in last glacial maximum sediment from Panama Basin in the eastern equatorial

*Author to whom correspondence should be addressed (yan.zheng@qc.edu).

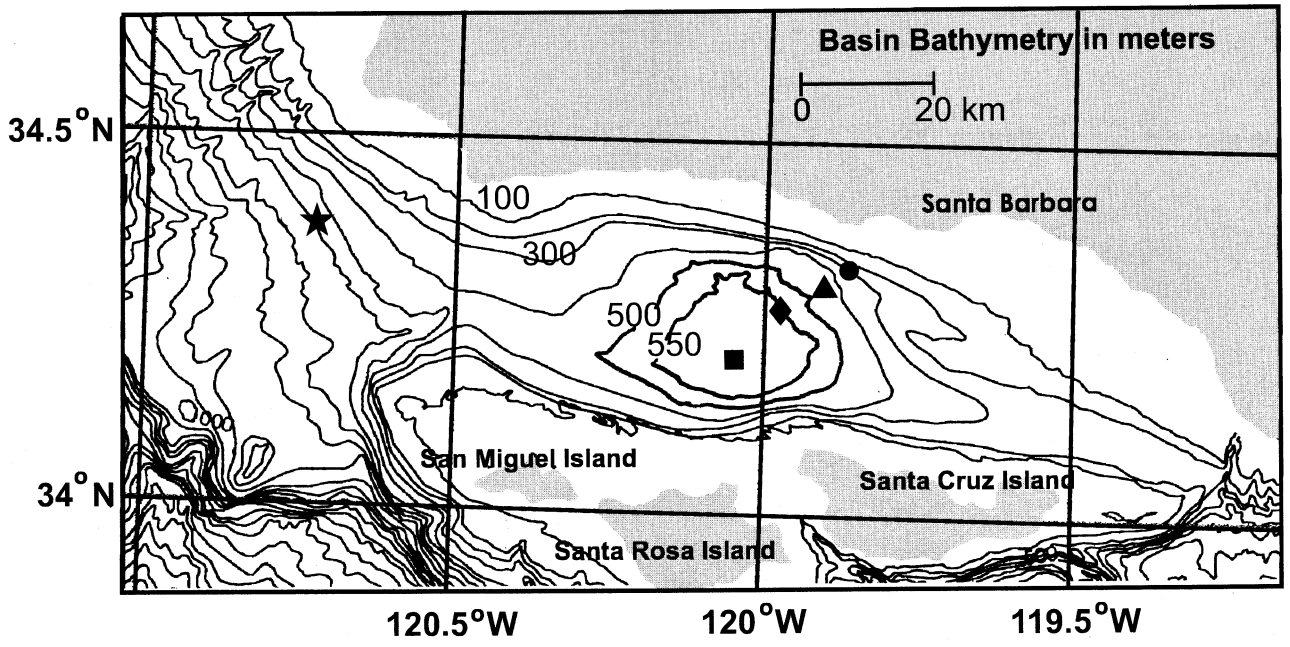

Fig. 1. Bathymetry of the Santa Barbara Basin, with location of multicores along the northeast flank of the basin. Cores M340-2 (340 m), M430-2 (430 m) and M580-2 (580 m) were recovered during a cruise in November/December 1995. Cores M440-3 (440m), M550-3 (550 m) and M590-3 (590 m) were recovered during a cruise in April 1997. Symbols on this map are used in later graphs to indicate data from corresponding sampling locations. The location of sediment trap deployed by Thunell et al. (1995) is almost exactly the same as cores M580-2 and M590-3 (square). The star symbol indicates the location where a dissolved oxygen profile was obtained outside of the basin (Fig. 2).

Pacific, on the other hand, has been interpreted as evidence against bottom water anoxia at the time (Pedersen et al., 1988).

Despite a substantial knowledge about Mo cycling in the ocean, many questions remain, particularly those related to the mechanism of Mo removal from the sea (Helz et al., 1996). Molybdenum is a biologically-essential element (Williams, 1994), but it is not known whether significant amounts of biogenic Mo exist in plankton matter, and whether it is easily regenerated from biogenic detritus if it exists. Another unresolved issue is the pathway leading to Mo enrichment in near anoxic sediment: scavenging onto Mn-oxides or diffusion to the underlying sediment followed by Mo sulfide precipitation. The mechanism leading to insoluble Mo formation is not clear. Molybdenum could be precipitated either following a reduction to Mo(IV), or without reduction. It is also unclear what roles sulfide plays in authigenic Mo formation. If Mo precipitation requires a reduction step, it is not known whether the reduction is microbially mediated or not.

In this study, a transect of sediment cores taken along the slope of the Santa Barbara Basin (SBB), where the bottom water oxygen ranges from near zero ($\sim$3 μM) to 25 μM, was used to address some of the remaining questions of Mo marine geochemistry, particularly its removal by sulfide-induced precipitation. The rain rate of particulate non-lithogenic Mo sinking through the water column is evaluated using sediment trap samples, while the diffusive flux of Mo into sediments is constrained using pore water concentration gradients. These sources are compared to the authigenic Mo accumulation rate to test for additional source or loss terms that may be unaccounted for. In this paper, the term "particulate non-lithogenic" is used to identify Mo that has become associated with particles in the water column, and to distinguish this source of Mo from "authigenic" Mo in sediments, which refers to non-lithogenic Mo from all sources, including precipitation in situ.

2. THE GEOCHEMICAL SETTINGS OF SANTA BARBARA BASIN

Santa Barbara Basin is a shallow, near-shore basin off southern California with suboxic conditions below the sill depth (Fig. 1). Below the basin sill depth of 475 m the water column is relatively quiescent with infrequent exchange with waters outside of the basin, as evidenced by the occurrence of water column nitrate depletion (Reimers et al., 1990).

Bottom water oxygen concentrations over the coring sites range from 3 to 25 μM (Fig. 2). Dissolved sulfide concentrations of the subsill water vary from 5 to 15 nM, detectable only by highly sensitive square-wave voltammetry (Kuwabara et al., 1999). Sediment recovered from the center of the basin is varved and has an accumulation rate of 0.4 cm/yr, or 92 g/cm^2 kyr (Soutar, 1971; Bruland et al., 1981; Kennett and Ingram, 1995; Behl and Kennett, 1996). Variable sediment input is the primary factor controlling varve formation, with dark laminae formed during fall-winter periods of high lithogenic flux and light laminae formed during spring-summer periods of high biogenic silica flux (Thunell et al., 1995). The organic carbon flux to the sediment is 2.8 g/cm^2 kyr (Thunell et al., 1995).

3. SAMPLING AND EXPERIMENTAL METHODS

During two cruises on board RV *Pt Sur* (November 30 to December 3, 1995, and April 25 to 27, 1997), six multicore deployments recovered undisturbed sediment from 4 sites at

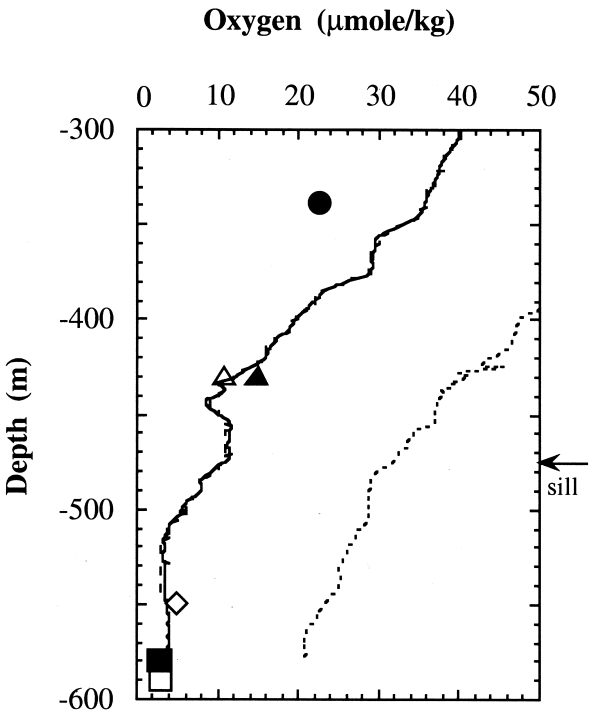

Fig. 2. Dissolved oxygen concentrations inside the Santa Barbara Basin (solid line: Nov./Dec. 95, dashed line: Apr. 97) and outside on the California Margin 90 km west of the basin (dotted line) measured by an oxygen sensor attached to the rosette-CTD on board R. V. *Pt. Sur*. Bottom water oxygen concentrations sampled from a Niskin bottled attached to the Multi-corer were determined by micro-Winkler titration for each site for both cruises (solid symbols, 1995; open symbols, 1997; Kuwabara et al., 1999). The profiles show that the water column of the Santa Barbara Basin is depleted in oxygen relative to the open California Margin above the sill depth (475 m, arrow) as well as in the deepest portion of the basin, partly due to restricted circulation of the basin water and partly due to the high biologic productivity of the basin surface water.

nominal depths of 340 m, 430 and 440 m, 550 m, and 580 and 590m (e.g., Table 1, Kuwabara et al., 1999, note that the core at depth 440 m is erroneously assigned as M430-3 in that paper). Cores M340-2, M430-2 and M440-3 (above the sill depth of 475 m) are designated as "slope" cores; and cores M550-3, M580-2 and M590-3 (below the sill depth of 475 m) are designated as "basin" cores. Bottom water oxygen concentrations sampled from a Niskin bottle attached to the multicorer were determined on board by micro-Winkler titration (Kuwabara et al., 1999).

Subsamples of a bi-weekly series of sediment trap samples collected between Aug. 1993 and Aug. 1994 (Thunell et al., 1995) together with the brine collected in the cup were provided for this study. The sediment trap was deployed in the center of SBB at 540 m depth, in 590 m of water. The sediment traps were poisoned with sodium azide (~11 g/L) and sodium borate (~0.25 g/L) was added for buffering. The brine samples were stored frozen in 50 mL centrifuge tubes and thawed after 3 yr of storage before ~7 mL subsamples were filtered through 0.45 μm syringe filters and acidified using Seastar HCl to pH ~2.

3.1. Sediment Collection and Subsampling

A standard multicorer (Barnett et al., 1984) was employed during both cruises to collect sediment cores. The core tube sampled for pore waters was immediately transferred to a refrigerated van cooled to the bottom water temperature of 6°C. Sectioning was carried out in a nitrogen-filled glove bag. The overlying water was sampled and filtered through a 0.45 μm acid-cleaned Millipore syringe filter inside the glove bag. Sediments were centrifuged in the cold van, then taken to another nitrogen-filled glove bag at room temperature where pore waters were filtered through 0.45 μm acid cleaned Millipore syringe filters. Sectioning, centrifuging and filtration took approximately 6 to 8 h. Filtered pore waters were acidified to pH ~2 by adding appropriate amounts of Seastar concentrated HCl (2 μL for every ml of pore water) after the samples were returned to the shore-based laboratory.

3.2. Chemical Analyses of Dissolved Constituents

Dissolved Mo concentrations in filtered and acidified pore waters, sediment trap brine samples, and sea water samples from SBB were determined by isotope dilution inductively coupled plasma-mass spectrometry (ID ICP-MS) using a procedure similar to that described by Colodner (1991) and by Toole et al. (1991). One hundred μL of water samples and an appropriate amount of isotope spike (^{94}Mo) were diluted to 10 mL in a matrix of 0.1% HNO_3 (Seastar) and equilibrated for over 24 h before measurement. The reproducibility is ~4%. A surface North Atlantic water sample analyzed together with SBB samples yielded a salinity normalized Mo concentration of 116 nM $\pm$ 3 nM (n = 4), comparable to previously published sea water Mo concentration values (Collier, 1985). Details for sampling and analysis of dissolved H_2S in pore waters from SBB by colorimetry and by square-wave voltammetry and pore water Fe by graphite-furnace atomic absorption spectrometry are described by Kuwabara et al. (1999).

3.3. Chemical Analyses of Solid Phase

Sediment solids from SBB were analyzed for Mo and Th, and radionuclides (^{210}Pb and ^{234}Th). All results of solid phase concentrations are normalized to salt-free values. The sediment samples were freeze-dried and ground using an agate mortar and pestle before analysis.

Molybdenum and Th in SBB sediment were determined by ID ICP-MS using ^{95}Mo and ^{236}U spikes (Zheng, 1999). The long term precision for measurement of both Mo and Th is ~4% based on 15 repeated analysis of a SBB sediment sample over one year. We obtained 1.52 $\pm$ 0.03 μg/g (n = 5) on a basalt standard BCR-1 with reported value of 1.6 μg/g. About 10 mg of sediment sample together with an appropriate amount of isotope spikes (^{95}Mo and ^{236}U) were digested in concentrated $HClO_4$, followed by concentrated HF and HNO_3, then re-dissolved in 1% HNO_3. Concentrations of Mo and Th in solution were measured using a VG Plasma Quad 2+ ICP-MS.

For ^{210}Pb analysis, sediments were dissolved in the presence of an isotopic yield monitor, after which the radionuclides were purified and plated onto silver disks for counting of ^{210}Po and ^{208}Po by alpha spectrometry following the method of Anderson et al. (1988). Excess ^{210}Pb (xs^{210}Pb) values were calculated by

Table 1. Unsupported Pb-210 and initial Th-234 inventories, and unsupported Pb-210 derived mass accumulation rates (MAR) in the SBB cores.

Core	Water Depth (m)	Inventory xsPb-210 (dpm/cm^2)	Inventory initial Th-234 (dpm/cm^2)	Focusing Factor[1]	MAR (g/cm^2 yr)	1σ MAR (g/cm^2 yr)[2]	Focusing-corr MAR (g/cm^2 yr)
M340-2	340	387	14	2.9	242	8	84
M430-2	430	103	13	0.8	77	3	101
M440-3	440	147	7	1.1	100	2	91
M550-3	550	216	14	1.6	72	2	45
M580-2	580	256	26	1.9	93	2	49
M590-3	590	76*	2	1.3	65	3	50
Expected Inventory from Sediment Trap deployed for ~ two months in Spring and Fall 1978 (Moore, 1981)		161	13				

* low value due to loss of ~12 cm core top

[1] focusing factor is defined as measured inventory of xsPb-210 divided by focusing-free inventory of xsPb-210, which is derived by comparison of sediment trap Th-232 flux and the sediment Th-232 accumulation rate in the deep basin (Zheng, 1999). It is assumed that the scavenging flux of Pb-210 is uniform throughout the study area.

[2] error is propagated from the error of slope of linear regression used to obtain MAR.

subtracting the background ^{210}Pb counted on samples at depth. Gamma spectrometry was used to measure the activity of ^{234}Th in samples from the uppermost few cm of each core, and the results were decay-corrected to the date of sampling to yield initial ^{234}Th values.

4. RESULTS

4.1. Sediment Trap Results

Solid phase Mo concentrations range from 2 to 3.4 μg/g with a flux-weighted average of 2.5 μg/g (Fig. 3a). There is on average an excess of 0.85 μg/g of Mo in the sediment trap solid phase when compared to the detrital background Mo value (Fig. 3a) derived from the Th concentration in the solid sample and a detrital Mo/Th ratio of 0.228 (g/g), based on average shale Mo and Th compositions (Wedepohl, 1978). Concentrations of Mo in brine samples were found to be up to 10 times greater than in seawater (Fig. 3a). When the released Mo is added to the solid phase Mo, the flux-weighted mean particulate non-lithogenic Mo becomes 1.27 μg/g. The origin of the particulate non-lithogenic Mo is unknown, but the fact that the supernant brines have dissolved Mn concentrations ~3 orders of magnitude greater than in intermediate depth water of the northeast Pacific ocean (Landing and Bruland, 1987) suggests that scavenging by Mn-oxides may have been a contributing factor.

4.2. Sediment ^{234}Th, ^{210}Pb, and Mass Accumulation Rate

Produced almost uniformly in the water column by ^{238}U decay, ^{234}Th ($t_{1/2}$ = 24.1 d) has the tendency to be scavenged onto particle surfaces. The presence of ^{234}Th with such a short half life within the top 1 to 2 cm of all sediment cores indicates that fresh material deposited within the past few months was recovered by coring (Figure 4). One deep basin core (M580-2) displays an inventory of 26 dpm/cm^2 (Table 1). In contrast, the other deep basin site (M590-3) has a very low inventory of 2 dpm/cm^2. Surficial sediment from the deep basin site at 590 m should have an xs^{210}Pb concentration of 70 to 90 dpm/g based on two previous studies (Koide et al., 1973; Bruland et al., 1981). This is consistent with our measurements at M580-2. The unsupported ^{210}Pb concentration in surficial sediment of M590-3, however, is only 37 dpm/g. The xs^{210}Pb profiles from cores M580-2 and M590-3 can be matched by shifting the xs^{210}Pb profile of M590-3 downward by 12 cm. This leads us to conclude that 12 cm of sediment was lost from M590-3. The presence of a small, but detectable ^{234}Th inventory and concentration (~10 dpm/g) at <1 cm depth in M590-3 (Fig. 4) indicates that the loss of surface sediment did not occur during coring, but some time between December 1995 and April 1997. The interpretation is consistent with a sequence of X-radiographs obtained from box cores over the same period (T. Baumgartner, pers. comm.). It is unclear whether this loss was due to a natural erosion event or dredging and sampling activities in this heavily sampled area.

Total sediment mass accumulation rates (MAR) range from 65 to 242 g/cm^2 kyr for SBB cores (Table 1), estimated using the slope (b) obtained on a linear best fit of ln($^{210}_{xs}$Pb) distribution with the cumulative mass (Fig. 4) (Ricketts and Anderson, 1998). The uncertainty in MAR is propagated from the standard error of the slope. M580-2 has a MAR (93 g/cm^2 kyr) equal to that estimated previously at a nearby site using $^{210}_{xs}$Pb (Bruland et al., 1981). Sediment MAR in SBB is influenced by sediment focusing, as evidenced by a factor of 4 range of $^{210}_{xs}$Pb inventories (Table 1), excluding the low value for perturbed core M590-3. Focusing-corrected sediment MAR at the slope sites (Table 1) are twice as high as those of the basin sites, consistent with the previous contention that near shore sites have higher lithogenic input than deep-basin sites (Schwalbach and Gorsline, 1985).

4.3. The Sediment Redox State

Deep basin sediments are characterized by an intense redox gradient within a few cm of the sediment-water interface, resulting in overlapping of oxic, suboxic and anoxic diagenetic reactions (Reimers et al., 1996). These features are observed at M580-2, which displays the shallowest Fe maximum among all the sites studied here, at 1.7 cm, and very high values of sulfide (Fig. 5). At this site, the sulfide concentration rises to >0.1

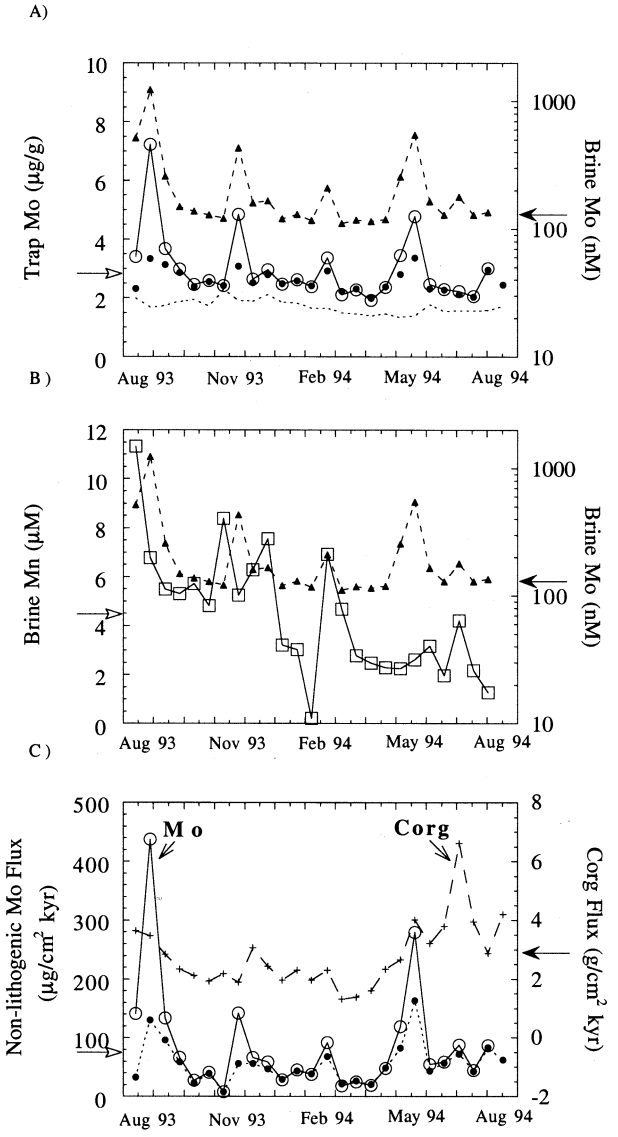

Fig. 3. a) Concentrations of Mo measured in two-week duration sediment trap solid (solid circles and lines) and brine (triangles and dashed lines) samples collected in Santa Barbara Basin during the period of August 1993 to August 1994 (Thunell et al., 1995). The open symbols indicate the solid phase Mo after adding the Mo mobilized into the brine. The thin dotted line indicates the detrital background level of Mo estimated from the Th concentration of the solids assuming a detrital end member Mo/Th ratio of 0.228 (g/g). Hollow arrow indicates the flux-weighted mean concentration of corrected Mo, at 2.9 μg/g. Solid arrow indicates the concentration of Mo ($\sim$120 nM) in SBB waters.b) Concentrations of Mn (square) and Mo (triangle) in sediment trap brine samples. The annual mean of sediment trap brine Mn concentration is 4.4 μM (indicated by hollow arrow), nearly three orders of magnitude higher than the Mn concentration of $\sim$10 nM in the OMZ waters of the eastern tropical Pacific (Landing and Bruland, 1987). Solid arrow indicates the concentration of Mo ($\sim$120 nM) in SBB waters.c) Time series of particulate non-lithogenic fluxes of Mo, both un-corrected (solid symbols) and corrected (open symbols). Hollow arrow indicates annual average rain rate of particulate non-lithogenic Mo, at 87 μg/cm^2 kyr. Time series of organic carbon flux to the basin (pluses, dash line) does not correspond very well with the non-lithogenic Mo fluxes. Solid arrow indicates annual average flux of organic carbon, at 2.8 g/cm^2 kyr.

μM right below the sediment water interface, reaches 100 μM less than 10 cm depth downcore (Fig. 5), and exceeds 1000 μM below 25 cm (Kuwabara et al., 1999). Less reducing conditions are found at the shallow basin site (550 m), where the maximum sulfide concentration is 0.05 μM at 10 cm (Fig. 5). The Fe peak at 550 m is also much broader than at 580 m (Fig. 5), suggesting less active removal of Fe at the shallower site by sulfide precipitation.

The sediment redox gradient is much weaker at the slope sites (Fig. 5), as shown by deeper Fe maxima and much lower sulfide concentrations. The maximum sulfide concentration is 0.02 to 0.04 μM at 10 cm downcore for the 430 m site, and is $<$0.005 μM at 10 cm downcore for 340 m site.

4.4. Pore Water and Solid Phase Mo

The degree of pore water Mo concentration deviation from bottom water follows the sediment redox gradient, with the largest depletion in the most reducing sediment in the deep basin, and the largest enrichment in the least reducing sediment on the slope. Substantial depletion of Mo throughout the core is observed only in M580-2 (Fig. 5). Pore water Mo concentrations in M580-2 decrease from the bottom water value of $\sim$120 nM to $\sim$80 nM at 2.3 cm downcore, and to $\sim$10 nM at 11 cm downcore (Fig. 5). At the shallower basin site (M550-3), pore water Mo concentrations are only slightly below bottom water values, and there is no systematic trend with depth in the Mo profile (Fig. 5). At the slope sites, pore water Mo concentrations are higher than bottom water values of $\sim$120 nM by 5 to 40 nM. Pore water Mo concentrations increase downcore at 340 m and at 430 m, more so at the shallower site.

Elevated pore water Mo concentrations in the upper 4 cm of core M590-3 may reflect a transient feature associated with dissolution of authigenic Mo following the loss of 12 cm core top. Further downcore in M590-3, pore water Mo concentrations follow a trend similar to that in M580-2, decreasing to $\sim$10 nM at 10 cm (Fig. 5).

Sedimentary authigenic Mo is found at all sites (Fig. 5), but concentrations reach much higher values (up to 30 μg/g) in the more reducing basin cores than in the slope cores ($\sim$1 μg/g). Sedimentary authigenic Mo is defined as Mo enrichment over its detrital background value, which is calculated using Th concentrations in the sediment and a detrital end member Mo/Th ratio of 0.228 (g/g). This detrital end member ratio is based on a detrital Mo concentration of 2 μg/g (Wedepohl, 1978) and a detrital Th concentration of 14.6 μg/g (Taylor and McLennan, 1985). The large number of samples from the upper 5 cm of M340-2 core without detectable authigenic Mo indicates that the average shale Mo/Th ratio provides an appropriate detrital end member for SBB, a conclusion further supported by results from sites along the open California continental slope (Zheng, 1999).

5. DISCUSSION

5.1. Mass Budget of Mo in SBB Sediments

A mass budget of authigenic Mo in SBB sediments is constructed based on the sediment authigenic Mo accumulation rate, the diffusive Mo flux calculated from Mo pore water concentration gradients, and the particulate non-lithogenic Mo

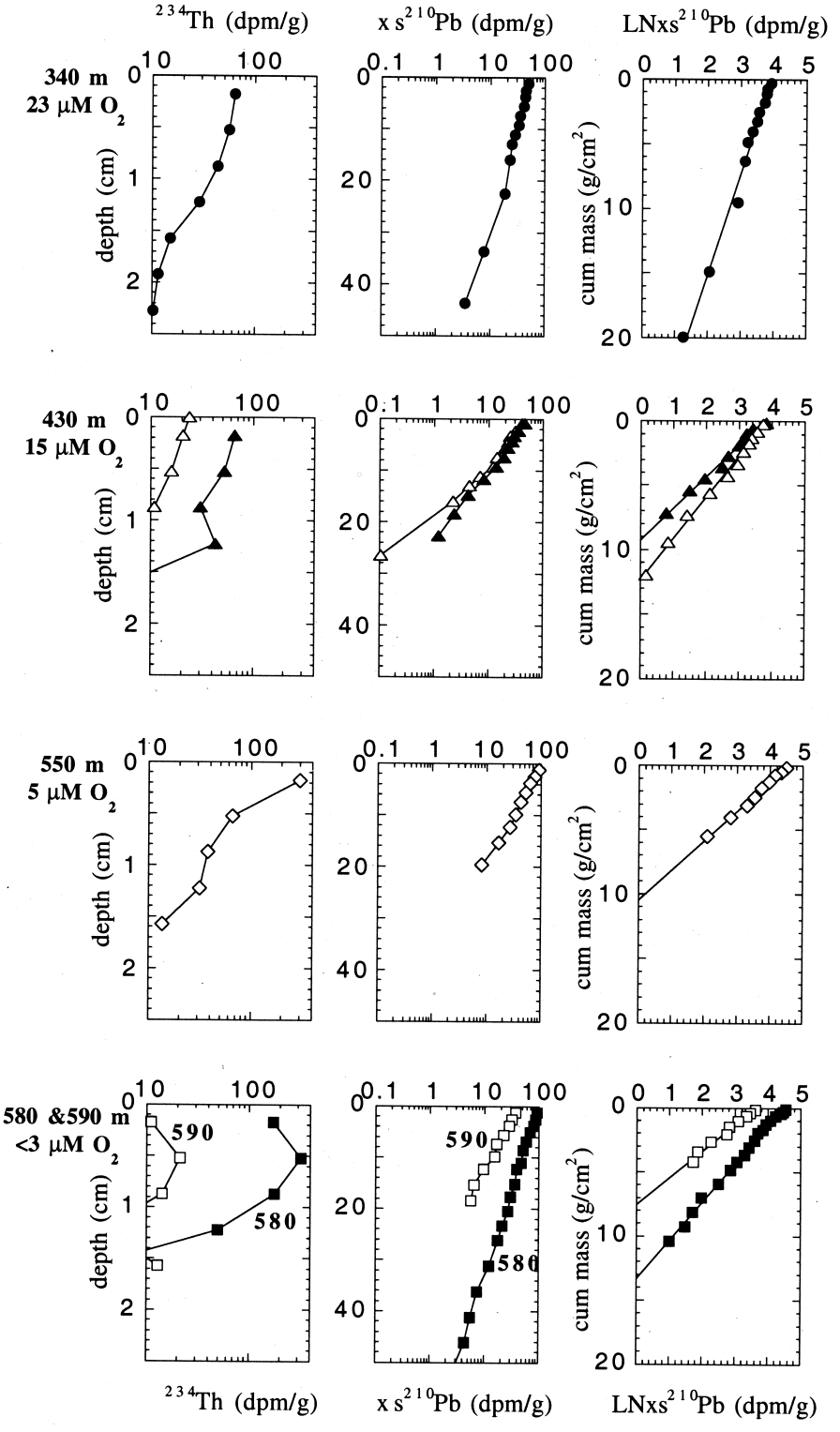

Fig. 4. Depth Profiles of initial ^{234}Th and un-supported ^{210}Pb. Data from Nov./Dec. 95 (M340-2, M430-2 and M580-2) and from Apr. 97 (M440-3, M550-3, M590-3) are shown by solid and open symbols, respectively. Measured ^{234}Th was decay corrected to the date of sample collection to yield initial ^{234}Th. Un-supported ^{210}Pb is also plotted with cumulative mass (the right column) to illustrate the inventory differences of each core, noticeably the high inventory at the 340 m site. The penetration depth of ^{234}Th is >2 cm in slope cores, while the penetration depth is <1.5 cm in basin cores, indicating reduced bioturbation in the basin cores. Low values of unsupported ^{210}Pb at the surface of core M590-3 together with the low un-supported ^{210}Pb inventory in this core suggests that sediment has been lost from the top of this core.

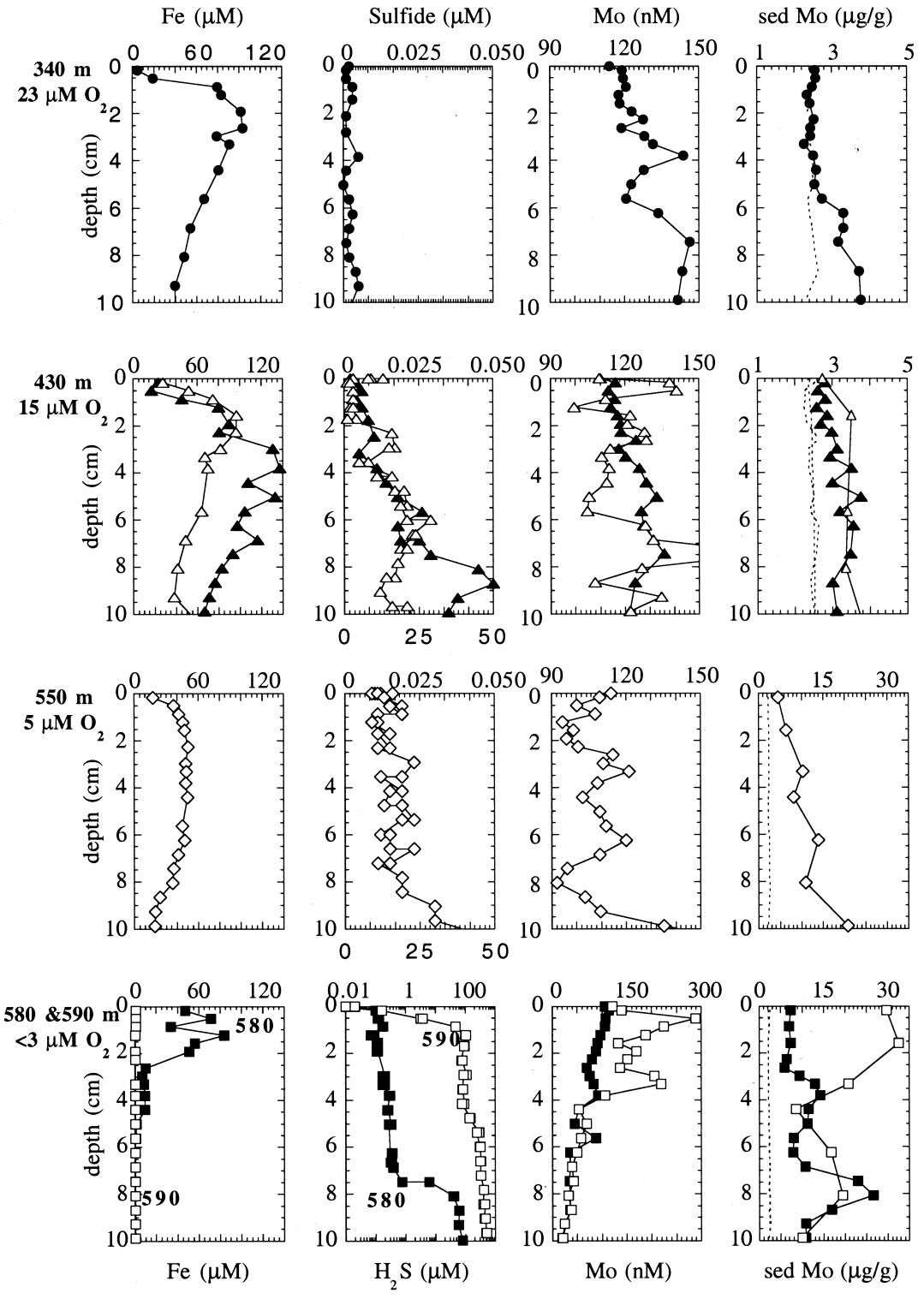

Fig. 5. Pore water profiles of dissolved Fe, sulfide and Mo in the upper 10 cm at four sites along the northeast flank of the Santa Barbara Basin, as well as the sedimentary Mo depth profiles where the dotted lines indicate the calculated detrital background values of Mo based on Th concentrations of the sediment assuming that the detritus has a Mo/Th ratio of 0.228 (g/g). The values for overlying water drawn at ~10 cm above the sediment-water interface are plotted at 0 cm in all pore water depth profiles. Notice the change to a log scale for sulfide at the 580/590 m site, and the scale for pore water Mo at this site is different as well. Sedimentary Mo scales are 0 to 35 μg/g for sites at 550 and 590 m, compared to 1 to 5 μg/g for sites at 340 and 430/440 m. Data from Nov./Dec. 95 (M340-2, M430-2 and M580-2) and from Apr. 97 (M440-3, M550-3, M590-3) are shown by solid and open symbols, respectively.

Table 2. Mo mass budget in the Santa Barbara Basin.

Core	Water Depth (m)	Oxygen (μM)[1]	Sulfide (μM)[2]	Avg. Mo_{auth}[3] (μg/g)	Sed Mo_{auth} MAR[4] (μg/cm^2 kyr)	Diffusive Mo Flux[5] (μg/cm^2 kyr)	Particulate Mo Flux[6] (μg/cm^2 kyr)
M340-2	340	23	0.005	1.2	290	−435	31
M430-2	430	15	0.040	0.7	52	−538	19
M440-3	440	11	0.025	1.0	97	−2413	37
M550-3	550	5	0.050	6.5	468	414	91
M580-2	580	3	100	13.6	1265	741	118
M590-3	590	3	500	12.9	839	N/A	83
Sediment Trap	540	—	—	—	—	—	87

[1] obtained by micro-Winkler titration of water collected by a niskin bottle attached to multi-corer
[2] pore water concentration at 10 cm depth in sediment
[3] average authigenic Mo concentration for sediment samples below the depths of Mo diagenesis (see text)
[4] burial rate of authigenic Mo estimated from average authigenic Mo concentrations below the zone of active diagenesis (see text) and sediment MAR (Table 1)
[5] calculated using equation (2) in section 5.1, positive flux indicates diffusion into sediment, negative flux indicates diffusion out of sediment. The imbalance between burial rate and diffusive flux, particularly at the slope sites, indicates that authigenic Mo formation at SBB is not at steady state.
[6] supply of particulate non-lithogenic Mo to sediments. For sites at 340, 430 and 440 m, the flux of particulate non-lithogenic Mo preserved and buried at each site is assumed to equal the sediment MAR multiplied by the authigenic Mo concentration in the shallowest sediment sample. For sites at 550, 580 and 590 m, it is estimated similarly, except that the concentration of particulate non-lithogenic Mo that is preserved and buried is 1.27 μg/g, as constrained by the annual average of the sediment trap samples.

input flux to the sediment evaluated using sediment trap samples.

5.1.1. Sediment authigenic Mo accumulation

The authigenic Mo mass accumulation rate (MAR, Table 2) is calculated using the following equation:

$$MAR_{Mo_{auth}} = [Mo_{auth}] \times MAR_{sed} \quad (1)$$

where MAR_{sed} is the sediment MAR (Table 1). To estimate authigenic Mo MAR, we adopt the average authigenic Mo concentration value for samples below the depth of active diagenesis for $[Mo_{auth}]$. The depth of active diagenesis is 6 cm for site M340-2, 4 cm for sites M430-2 and M440-3, and 10 cm for basin sites.

5.1.2. Diffusive input flux

The diffusive flux of Mo into the sediment is calculated from the pore water Mo concentration gradient with the following equation:

$$Flux = -\frac{DMoO_4^{4-}\,(6°C)}{\phi^2}\frac{\Delta Mo}{\Delta z} \quad (2)$$

Diffusivity of dissolved Mo in sediment has not been measured. The molecular diffusivity at 6°C (bottom water temperature of SBB) is calculated to be 5.82×10^{-6} cm^2/s based on the diffusivity at 25°C estimated by Li and Gregory (1974), and the temperature dependence equation (Stokes-Einstein relationship) described in Li and Gregory (1974); ø is porosity; $\Delta Mo/\Delta z$ is the pore water Mo gradient near the sediment water interface. The pore water gradient of Mo is calculated by taking the difference between the first sampling point in sediment and the overlying water, divided by the first sampling depth (Δz = 0.17 cm). At basin site M580-2, the Mo diffusive flux into the sediment (741 μg/cm^2 kyr; Table 2) is estimated by using the gradient between the first and second sampling points in pore water because the bottom water value obtained from this core appeared to be too low. The uncertainty in the calculated diffusive flux derives primarily from the need to estimate the concentration gradient at the sediment-water interface, using results from discrete depths. It is difficult to quantify this uncertainty, which could be as large as 50%. No diffusive Mo flux is calculated at perturbed site M590-3. There is an apparent Mo diffusive flux into the sediment at basin site M550-3 of 414 μg/cm^2 kyr (Table 2). However, pore water sulfide concentrations are low (<0.05 μM) at the 550 m site, and the pore water Mo profile is highly irregular (Fig. 5), suggesting that the authigenic Mo formation is not an ongoing process at the site (see discussion 5.2).

5.1.3. Particulate input flux

The annual particulate non-lithogenic Mo rain rate, after correcting for Mo released to the supernant, amounts to 87 μg/cm^2 kyr (Fig. 3c). The contribution of particulate non-lithogenic Mo to sediment authigenic Mo MAR is probably not uniform within the SBB, due to: 1) less preservation or less rain rate of particulate non-lithogenic Mo at the slope sites; and 2) pronounced and variable amounts of sediment focusing (Table 1). To evaluate this contribution, we assume that particles redistributed laterally by sediment focusing have a particulate non-lithogenic Mo content equal to that of the surface-most sample of each core at the slope sites, or equal to that of annual-average (1.27 μg/g) sediment trap samples at the basin sites. Then we multiply this preserved and buried particulate non-lithogenic Mo concentration by the sediment MAR to obtain the particulate non-lithogenic Mo flux to each site (Table 2). At the slope sites, the fluxes of particulate non-lithogenic Mo are <40 μg/cm^2 kyr (Table 2).

At the basin site M580-2, the diffusive flux of Mo into the sediments (741 μg/cm^2 kyr; Table 2) is 5 times greater than the flux of particulate non-lithogenic Mo (118 μg/cm^2 kyr; Table 2), and is within a factor of 2 of the current authigenic Mo

MAR (1265 μg/cm^2 kyr; Table 2). Diffusion of Mo into sediments, followed by precipitation in situ, must therefore be the dominant process supplying Mo to the basin sediments. At the slope sites, large negative diffusive fluxes of Mo (Table 2) indicate remobilization of Mo. The source of the remobilized Mo could be the particulate non-lithogenic Mo ($<$40 μg/cm^2 kyr; Table 2) supplied currently, or authigenic Mo that was formed in the sediment previously at a time when conditions in SBB were more reducing (see discussion 5.4).

5.2. Authigenic Mo Formation Mechanism: The Role of Sulfide

The master variable regulating Mo precipitation and regeneration seems to be the concentration of sulfide in pore waters. Two threshold levels of dissolved sulfide seem to be prerequisites for the formation of large amounts of authigenic Mo, as indicated by the trend observed in pore water and sediment Mo profiles from the depth transect of sediment cores from SBB. A first critical sulfide value appears to be $\sim$0.1 μM. This value is chosen based on a smooth decrease of pore water Mo concentration from the bottom water value of $\sim$120 nM to $<$60 nM at $\sim$3 cm depth in core M580-2, indicating active Mo precipitation through this interval (Fig. 5). Active Mo precipitation is also supported by the elevated sediment Mo concentration of 7.4 μg/g at the very surface of the sediment at 580 m, which is not bioturbated (Fig. 5). Yet throughout this interval, pore water sulfide concentrations remain close to $\sim$0.1 μM (Fig. 5), indicating that this level is sufficient for Mo precipitation.

A second critical level of $\sim$100 μM sulfide appears to trigger a depletion of pore water Mo to concentrations $<$10 nM downcore in M580-2 and M590-3. The loss of the surface sediment at the site of M590-3 fortuitously allows us to better constrain the second critical sulfide level. The most dramatic change of pore water Mo concentrations in M590-3 occurs at $\sim$3.8 cm, below which pore water Mo concentrations decrease rapidly with depth (Fig. 5). In conjunction with this Mo removal, the pore water sulfide concentration increases abruptly from $\sim$100 μM to $\sim$300 μM at $\sim$5 cm (Fig. 5). Above 3.8 cm, pore water sulfide concentrations are less than 100 μM and the exposed authigenic Mo ($\sim$40 μg/g) that was formed and buried deep in the sediment is dissolving, thereby elevating the pore water Mo concentration to 3 times that of the bottom water ($\sim$120 nM). This could be explained by dissolution of a Mo-sulfide phase that is only thermodynamically stable when the sulfide concentration is greater than 100 μM. The second critical sulfide level therefore appears to be somewhere between 100 μM to 300 μM.

It is possible that the form of authigenic Mo precipitated at the lower threshold level of sulfide ($\sim$0.1 μM) is different from the authigenic Mo formed at the higher threshold level of sulfide ($\sim$100μM). Comparison of Fe and Mo pore water profiles indicates that Fe is completely precipitated by $\sim$5 cm down core in M580-2, while substantial Mo removal is still ongoing at greater depth. This suggests that Mo-sulfide coprecipitation with Fe-sulfide is a viable mechanism when the sulfide concentration is low ($\sim$0.1 μM). In addition, pore water sulfide and Mo profiles in cores M580-2 and M590-3 indicate that precipitation of Mo continues after Fe is completely removed and sulfide concentrations rise above 100 μM (Fig. 5). Helz et al. (1996) hypothesized that removal of Mo occurred either as Mo-sulfide or as particle-bound Mo at threshold levels of sulfide between 50 to 250 μM. Our observations are consistent with either mechanism.

Although the sedimentary authigenic Mo concentrations at the 550 m site are nearly as high as at the 580 m site (Fig. 5), the pore water Mo profile at 550 m fails to show the extensive depletion seen at 580 m, possibly reflecting a relaxation from a previous more reducing condition (section 5.4). The lack of a large pore water Mo depletion at 550 m, and no consistent downcore depletion to $<$10 nM, suggests that formation of authigenic Mo was not active at this site during the few weeks before the April 1997 cruise when the sulfide concentrations were below 0.025 μM throughout the upper 8 cm. While the pore water Mo profile in this depth interval suggests that there were intermittent zones of Mo precipitation, clearly there was not the extensive depletion of dissolved Mo that was observed at the 580 m site (Fig. 5).

Several factors could contribute to the "spikiness" of Mo pore water profiles in both basin and slope cores (Fig. 5). These include: 1) the profiles reflect relaxation from previous more reducing conditions (section 5.4); 2) the irregularities reflect "micro zones" of sulfate reduction and sulfide oxidation, where Mo minima are associated with maxima of sulfate reduction, and Mo maxima are associated with maxima of sulfide oxidation; or 3) there may be unknown sampling artifacts. The "spikiness" of pore water Mo profiles seems to be a common feature that is also observed in several other California Borderland Basins and in the Chesapeake Bay (Shaw et al., 1990; Colodner, 1991).

5.3. Authigenic Mo Formation: The Role of Microbes

A comparison of Mo data for a series of anoxic basins (Cariaco, Saanich, SBB and, perhaps, Framvaren Fjord) suggests that authigenic Mo MAR is more sensitive to carbon flux than to bottom water sulfide concentration. The authigenic Mo MAR is $>$7000 μg/cm^2 kyr in Saanich Inlet with 30 μM H_2S, $\sim$700 μg/cm^2 kyr in the Cariaco Basin with 50 μM H_2S, $\sim$240 μg/cm^2 kyr in the Black Sea with 400 μM H_2S, and $\sim$1200 μg/cm^2 kyr in Framvaren Fjord with 8000 μM H_2S (Table 3). However, because the Mo concentration in the Black Sea water column has greatly decreased to $\sim$5 nM, and the Mo concentration in Framvaren Fjord has decreased to $\sim$20 nM, these basins are not easily included in this comparison. For Saanich Inlet and the Cariaco Basin with comparable bottom water concentrations of Mo and sulfide, much more authigenic Mo is formed in Saanich Inlet where the carbon flux is higher (5.7 g/cm^2 kyr) than the Cariaco Basin where the carbon flux is lower (0.7 g/cm^2 kyr). Furthermore, the authigenic Mo MAR at the basin sites (550 and 580 m) in the Santa Barbara Basin where the concentration of sulfide in bottom water is $\ll$1 μM but the organic carbon flux is 2.8 g/cm^2 kyr is comparable to that of the permanently anoxic Cariaco Basin (Table 3).

There are two possible explanations for the apparent relation between the organic carbon flux and authigenic Mo MAR in basins where water column Mo is not significantly depleted. The first is that organic carbon, the food source for sulfate-reducing bacteria, controls pore water sulfide concentrations

Table 3. Authigenic Mo mass accumulation rate in anoxic basins.

Basin	Carbon Flux (g/cm^2 kyr)[1]	Sulfide (μM)[2]	Bottom Water Mo (nM)[3]	Auth Mo MAR ($\mu g/cm^2$ kyr)[4]	Auth Mo ($\mu g/g$)[5]
Supply limited by bottom water depletion					
Framvaren Fjord	2	8000	20	1170	130
Black Sea	0.9	400	5	239	48
Supply not limited					
Cariaco Basin	0.7	50	90	713	57
Saanich Inlet	5.7	30	90	7719	81
Santa Barbara Basin	2.8	0	120	500–1200	10

[1] Sediment trap flux at the deepest water depth, refs for each basin in sequence are:
NÆS (1988), Muramoto (1991), Thunell (unpublished data), Anderson (1989) and Thunell (1995)
[2] maximum concentration in bottom water (Saanich Inlet is seasonally anoxic):
Skei (1988), Murray (1989), Scranton (1987), Crusius (1996), and Kuwabara (1998)
[3] Refs for Mo concentration in bottom water of each basin in sequence are:
Emerson and Huested (1991); Zheng (unpublished data for Santa Barbara)
[4] Refs for sediment MAR for each basin in sequence are:
NÆS (1988), Anderson (1991), Anderson (1987) & Dean (1999), Anderson (unpublished data), and this study
[5] Refs for sediment authigenic Mo concentration for each basin in sequence are:
Crusius (1996), Ravizza (1991) & Crusius (1996), Crusius (1996) & Dean (1999), Francois (1988), Crusius (1996), and this study.

near the sediment-water interface and therefore the rate of in situ precipitation of authigenic Mo. The second explanation, based on laboratory observations by Tucker et al. (1997), is that sulfate-reducing bacteria also reduce Mo(VI) to Mo (IV) and, therefore, that an increase in organic carbon determines the formation of authigenic Mo by controlling the activity of these bacteria. The available pore water sulfide data from these anoxic basins are insufficient to test these two pathways. Whichever mechanism applies, our compilation demonstrated that the accumulation rate of authigenic Mo in marine sediments depends as much on the rain of organic matter to sediments as on the sulfide concentration of bottom waters, and perhaps more so.

5.4. Authigenic Mo Response to Changing Redox Conditions in SBB

Variations in the redox conditions of the Santa Barbara Basin bottom waters (Figure 6d) are manifestations of circulation and climatic events outside of the basin (Reimers et al., 1996) and possibly, the El Nino Southern Oscillation (ENSO). Flushing of SBB appears to be relatively weak during the El Niño years, as indicated by low oxygen and nitrate concentrations of the deep basin waters (CalCOFI time series; Fig. 6d) corresponding to the several moderate positive sea surface temperature anomalies between 1990 and 1994 (NINO3 index; Fig. 6c). The linkage between SBB bottom water redox state and ENSO lies in how the basin water is ventilated: upwelling brings denser water to sill depth which can then spill over to ventilate the basin (Reimers et al., 1990), but suppression of the thermocline during El Niño years reduces upwelling intensity (Cane, 1996) and therefore ventilation of the SBB.

Sediment redox conditions, notably the sediment pore water sulfide concentrations, responded to changes in the redox conditions of the SBB bottom waters. Reimers et al. (1996) reported that during four cruises in February, June and October 1988, and later in June 1991, sediment pore water sulfide concentrations at deep basin sites reached 10 μM at down core depths of ~3 cm. In contrast, Kuwabara et al. (1999) showed that sulfide concentrations did not reach 10 μM until ~8 cm downcore in February and December 1995. A spill-over event occurred in May 1988, causing the basin to ventilate (Fig. 6d). However, the pore water sulfide values remained high in June and October 1988 (Reimers et al., 1996), suggesting that there might be a lag of sediment redox state response to the basin bottom water redox conditions.

Accumulation of authigenic Mo at the deep basin site (580 m) varied in response to the changing redox conditions of SBB bottom waters. Three large peaks of authigenic Mo concentration in the downcore record of M580-2 and M590-3 occurred at years 1972 $\pm$ 3, 1982 $\pm$ 1 and 1990 $\pm$ 1 (Fig. 6b). The most recent Mo peak (15 μg/g; 1990 $\pm$ 1) reflects the reducing conditions of the bottom water of SBB from 1990 through 1992 (Fig. 6d), and corresponds to small SST anomalies as well (Fig. 6c). Unfortunately, the CalCOFI time series does not extend back far enough for a direct comparison with the 1972 $\pm$ 3 (Mo 40 μg/g) and 1982 $\pm$ 1 (Mo 28 μg/g) peaks. But, these two time periods are intense El Niño years with significant SST anomaly greater than 2.5°C (Fig. 6c) and, therefore, presumably SBB could have been more reducing. This comparison shows that the concentration of authigenic Mo in SBB sediments could perhaps be used as a qualitative proxy for past redox conditions in the deep basin, and therefore for the reconstruction of past ENSO cycles.

In a system with varying redox conditions, one might expect authigenic Mo precipitated under more reducing conditions to be later remobilized when conditions become less reducing. Our results from SBB constrain the conditions under which authigenic Mo is remobilized as well as precipitated. Although conditions in 1995 were less reducing than those that existed in mid-1991 and in early 1988 (see above and Fig. 6d), conditions at the site of deep basin core M580-2 remained sufficiently reducing that pore water profiles of Mo show no evidence for remobilization of authigenic Mo from surface sediments (Fig. 5). Rather, precipitation of Mo remained active at this site,

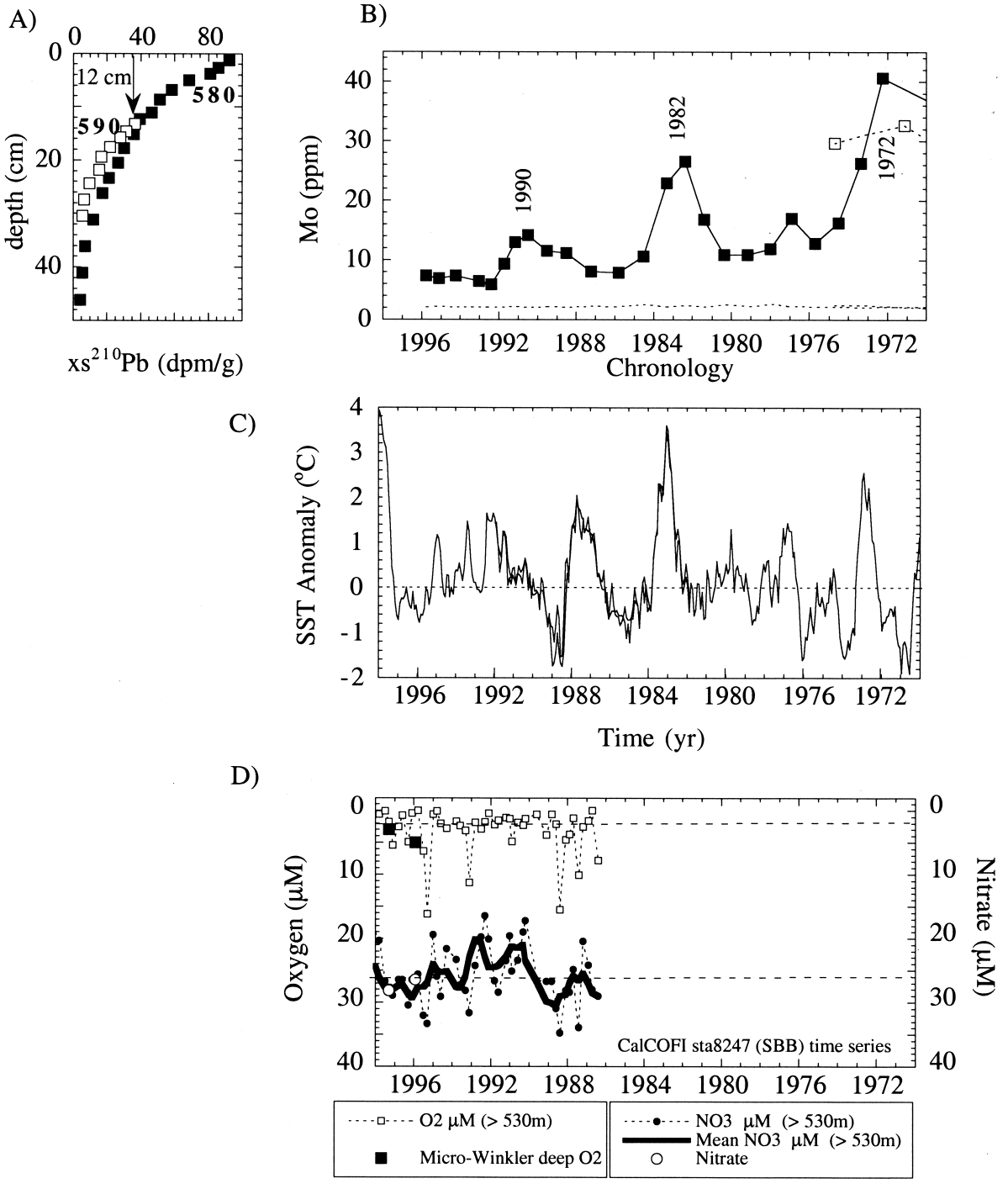

Fig. 6. a) Comparison of depth profiles of un-supported ^{210}Pb between cores M590-3 (open square) and M580-2 (solid square) after the depth scale of core M590-3 was shifted downward by 12 cm.b) After the depth adjustment on core M590-3, both deep basin cores showed a Mo peak of ~40 μg/g occurring at year 1972 $\pm$ 3, increasing our confidence in the ^{210}Pb chronology. Additional Mo peaks were also observed in core M580-2 in y 1982 $\pm$ 1 and 1990 $\pm$ 1. The dotted line without symbols indicates the calculated detrital background values of Mo based on Th concentrations of the sediment assuming that the detritus has a Mo/Th ratio of 0.228 (g/g).c) NINO3 monthly-averaged sea surface temperature anomaly in the eastern equatorial Pacific obtained from a blend of ship, buoy, and bias-corrected satellite data from the Integrated Global Ocean Services System web page (http://ingrid.ldgo.columbia.edu/SOURCES/.Indices/ensomonitor.html). d) Variation in oxygen and nitrate concentrations of Santa Barbara Basin subsill waters (>500 m). Except for values determined during cruises in this study (open circle and closed square), these data are from the CalCOFI station 82.47 time series from 1986 to 1998. Bottom water oxygen concentrations during the cruises were determined by Micro-Winkler titration (J. Bernhard, unpublished).

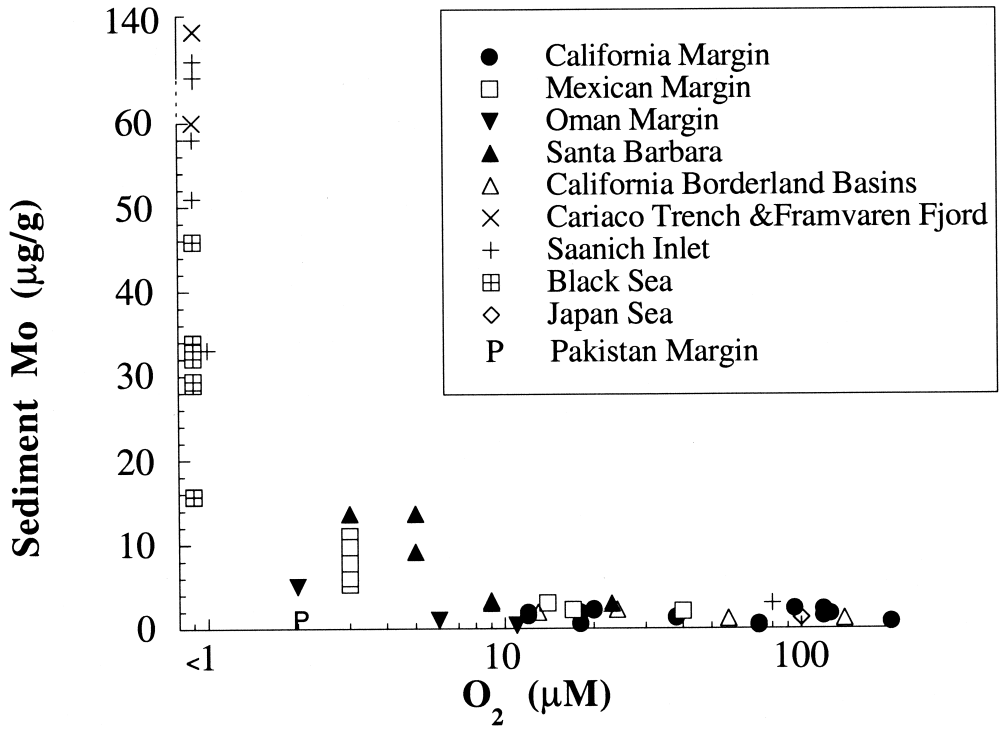

Fig. 7. A compilation of sedimentary Mo concentrations show that enrichment of Mo is dependent on the oxygen concentration of the bottom water. Mo data are from the California Margin (Zheng unpublished data); Mexican Margin (Nameroff, 1996); Oman Margin (Morford and Emerson, 1999); Pakistan Margin (Crusius et al., 1996) and near shore ocean basins (Saanich Inlet: Francois, 1988; Crusius et al., 1996; Black Sea: Crusius et al., 1996; Ravizza et al., 1991; Japan Sea: Crusius et al., 1996; Cariaco Basin: Emerson and Huested, 1991; Framvaren Fjord: Emerson and Huested, 1991; Santa Barbara Basin: this study; and other California Borderland Basins (Patten Escarpment, San Clemente, Santa Cruz and San Nicholas): Zheng unpublished data). Compilation excludes sediments in which Mo enrichments are believed to be associated with Mn oxyhydroxides (Shimmield and Price, 1986; Shaw et al., 1990). Cores with high Mn concentrations have also been excluded from the California Borderland Basin data.

albeit at a rate lower than that which existed previously when conditions were more reducing.

The varying redox conditions of SBB might also be responsible for the absence of the Mo peak one would expect to find corresponding to the 1987 ENSO event. A relatively large negative SST anomaly in 1988 (Fig. 6c) might have caused strong flushing of SBB as indicated by high nitrate values in May 1988 (Fig. 6d). The oxygenation of SBB could have caused remobilization of authigenic Mo deposited during the 1987 El Niño year. Therefore, concentration maxima of authigenic Mo in SBB sediment indicate that an El Niño event has occurred, but because of the potential for remobilization of authigenic Mo, the absence of an authigenic Mo peak does not suggest that an El Niño event has not occurred.

In contrast to the deep basin site, the less reducing conditions encountered in 1995 and 1997 had an impact on Mo geochemistry at the shallow basin (M550-3) site. Concentrations of authigenic Mo in excess of 15 μg/g in sediments of the shallow basin site (Fig. 5) indicate the existence of active Mo precipitation at some time in the recent past, although the absence of strong depletion of Mo in pore waters indicates that intense precipitation of authigenic Mo was not occurring at the time of sampling in 1997. While a change in redox conditions has led to a decline in the rate of authigenic Mo formation at the shallow basin site, there is no evidence for extensive remobilization of authigenic Mo either. Redox conditions are poised at a level where neither precipitation nor remobilization dominates the flux of Mo at the shallow basin site. The diffusive flux of Mo out of sediments at 340 m and 430 m (Table 2 and Fig. 5) indicates regeneration of authigenic Mo under redox conditions that existed at the time these sites were sampled.

5.5. Authigenic Mo as Paleo-Anoxia Proxy

The Santa Barbara Basin depth transect of cores clearly demonstrates that formation and preservation of authigenic Mo requires the presence of sulfide close to the sediment water interface, at a concentration greater than 0.1 μM. This very reducing condition is achieved under highly productive waters of SBB only when the bottom water oxygen concentration is less than 10 μM (Fig. 5). There are very few places in the ocean where the biologic productivity surpasses that of the SBB (Eppley and Peterson, 1979; Platt, 1985). In the cases where the biologic productivity is less than that of SBB, authigenic Mo precipitation probably requires anoxic bottom water, as in the case of the Cariaco Basin (Dean et al., 1999). Sediments from SBB slope sites bathed in waters with >10 μM showed very little authigenic Mo precipitation, even if the carbon flux reaching these sites is the same as the flux reaching the sites of the basin cores. Therefore, there is a clearly an empirical relation

between bottom water oxygen and authigenic Mo formation, at least within SBB.

This empirical relation between sedimentary authigenic Mo and bottom water oxygen concentration is further supported by a compilation of data from various locations (Fig. 7). Except in Pakistan margin sediments (Crusius et al., 1996), sedimentary Mo is found to be 5 to 140 μg/g when the overlying water oxygen concentration is less than 10 μM. At present we do not understand why there is no authigenic Mo enrichment in Pakistan margin sediments because we would expect levels there to be similar to maximum values of $\sim$30 μg/g observed in surface sediments located in the oxygen minimum zone at the nearby Indian margin (Sirocko, 1995). We also realize that the empirical relationship between authigenic Mo and bottom-water oxygen concentration is indirect, and is established via non-linear relationship between oxygen and pore water sulfide. Further tests of this relationship under settings where both bottom water oxygen concentration and carbon flux are high are needed. With the above caveats, we propose the following two interpretations for past authigenic Mo enrichments: 1) enrichment of Mo indicates the presence of sulfide in bottom waters; or 2) the presence of authigenic Mo indicates a combination of low bottom water oxygen ($<$10 μM) and high carbon flux, similar to modern conditions in the SBB and on the Mexican and Oman margins.

6. CONCLUSIONS

Concentrations of pore water sulfide control the formation of authigenic Mo in marine sediments. There are two critical dissolved sulfide concentrations for authigenic Mo formation. The first critical value is $\sim$0.1 μM, where authigenic Mo formation starts, probably by co-precipitation of a Mo-Fe-S phase. Pore water and solid phase Mo data from Santa Barbara Basin indicate negligible formation of authigenic Mo at sulfide concentrations below 0.1 μM. The second critical value is $\sim$100 μM, where direct Mo-sulfide precipitation or the switching of Mo behavior from conservative to particle reactive occurs. If Mo is removed by Mo-sulfide precipitation, then the second critical value of sulfide is dependent on the concentration of Mo as the solubility product must remain constant at given temperature and pressure.

The linkage of authigenic Mo formation with sulfide can be exploited for paleo-reconstruction because often such conditions require bottom water anoxia, or bottom water near anoxia ($<$10 μM O_2) and high carbon flux.

A mass budget of Mo for the deep SBB site (580 m) demonstrates that the dominant source of the sedimentary authigenic Mo is precipitation in situ of Mo supplied by diffusion from bottom waters, with at most 15% derived from particulate non-lithogenic Mo input.

Acknowledgments—We thank Renee Takesue and marine technicians Richard Muller and Charles Cheany of R.V. *PtSur* for valuable assistance at sea. Rosanne Schwartz made the ^{210}Pb analyses. Dr. Robert Thunell kindly provided the sediment trap and brine samples, and shared unpublished results from Cariaco Trench. The ICP-MS facility at LDEO is managed by Rick Mortlock. The manuscript also benefited from thorough reviews by Dr. G. Ravizza and an anonymous reviewer. The cruises were funded by NSF through OCE-94-17038 to A. van Geen, with additional support for analyses provided by OCE-93-14634 to R. F. Anderson. Support to J. Kuwabara for sulfide analyses was provided by the Toxic Substances Hydrology Program of the USGS. LDEO contribution number 6071.

Associate editor: B. P. Bovdreau

REFERENCES

Anderson R. F. (1987) Redox behaviors of uranium in an anoxic marine basin. *Uranium.* **3,** 145–164.

Anderson R. F., Bopp R. F., Buesseler K. O., and Biscaye P. E. (1988) Mixing of particles and organic constituents in sediments from the continental shelf and slope off Cape Cod: SEEP-I results. *Continental Shelf Research.* **8,** 925–946.

Anderson R. F. and Fleisher M. Q. (1991) Uranium precipitation in Black Sea sediments. In *Black Sea Oceanography* (ed. E. Izdar and J. W. Murray), pp. 443–458. Kluwer Academic Publishers.

Anderson R. F., LeHuray A. P., Fleisher M. Q., and Murray J. W. (1989) Uranium deposition in Saanich Inlet sediments, Vancouver Island. *Geochim. Cosmochim. Acta.* **53,** 2205–2213.

Barnett P. R. O., Watson J., and Connelly D. (1984) A multicorer for taking virtually undisturbed samples from shelf, bathyal, and abyssal sediments. *Oceanologica Acta.* **7,** 399–408.

Behl R. J. and Kennett J. P. (1996) Brief interstadial events in the Santa Barbara Basin, NE Pacific, during the last 60 kyr. *Nature.* **379,** 243–246.

Berrang P. G. and Grill E. V. (1974) The effect of manganese oxide scavenging on molybdenum in Saanich Inlet, British Columbia. Mar. Chem. **2,** 125–148.

Bertine K. K. and Turekian K. K. (1973) Molybdenum in marine deposits. *Geochim. Cosmochim. Acta.* **37,** 1415–1434.

Bruland K. W., Franks R. P., and Landing W. M. (1981) Southern California inner basin sediment trap calibration. *Earth Planet. Sci. Lett.* **53,** 400–408.

Brumsack H. J. and Gieskes J. M. (1983) Interstitial water trace-metal chemistry of laminated sediments from the Gulf of California, Mexico. *Mar. Chem.* **14,** 89–106.

Calvert S. E. and Price N. B. (1977) Geochemical variation in ferromanganese nodules and associated sediments from the Pacific Ocean. *Mar. Chem.* **5,** 43–74.

Cane M. A. (1996) El Nino. *Annu. Rev. Earth Planet. Sci.* **14,** 43–70.

Collier R. W. (1985) Molybdenum in the Northeast Pacific Ocean. *Limonol. Oceanogr.* **30(6),** 1351–1354.

Colodner D. (1991) The Marine Geochemistry of Rhenium, Iridium and Platinum. Ph.D., Woods Hole Oceanographic Institution Massachusetts Institute of Technology.

Colodner D., Edmond J. and Boyle E. (1995) Rhenium in the Black Sea: comparison with molybdenum and uranium. *Earth Planet. Sci. Lett.* **131,** 1–15.

Crusius J., Calvert S., Pedersen T., and Sage D. (1996) Rhenium and molybdenum enrichments in sediments as indicators of oxic, suboxic and sulfidic conditions of deposition. *Earth Planet. Sci. Lett.* **145,** 65–78.

Dean W. E., Piper D. Z., and Peterson L. C. (1999) Molybdenum accumulation in Cariaco basin sediment over the past 24 k.y.: A record of water-column anoxia and climate. *Geol.* **27,** 507–510.

Emerson S. R. and Huested S. S. (1991) Ocean anoxia and the concentration of molybdenum and vanadium in seawater. *Mar. Chem.* **34,** 177–196.

Eppley R. W. and Peterson B. J. (1979) Particulate organic matter flux and planktonic new production in the deep ocean. *Nature.* **282,** 677–680.

Francois R. (1988) A study on the regulation of the concentrations of some trace metals (Rb, Sr, Zn, Pb, Cu, V, Cr, Ni, Mn and Mo) in Saanich Inlet sediments, British Columbia. Mar. Geol. **83,** 285–308.

Helz G. R., Miller C. V., Charnock J. M., Mosselmans J. F. W., Pattrick R. A. D., Gardner C. D., and Vaughan D. J. (1996) Mechanism of molybdenum removal from the sea and its concentration in black shales: EXAFS evidence. *Geochimica Cosmochimica Acta.* **60(19),** 3631–3642.

Jacobs L., Emerson S., and Huested S. S. (1987) Trace metal geochemistry in the Cariaco Trench. *Deep Sea Res.* **34,** 965–981.

Kennett J. P. and Ingram B. L. (1995) A 20,000 year record of ocean

circulation and climate change from the Santa Barbara Basin. *Nature.* **377,** 510–513.
Koide M., Bruland K. W., and Goldberg E. D. (1973) Th-228/Th-232 and Pb-210 geochronologies in marine and lake sediments. *Geochim. Cosmochim. Acta.* **37,** 1171–1187.
Kuwabara J. S., Geen A. V., McCorkle D. C., and Bernhard J. M. (1999) Dissolved sulfide distribution in the water column and sediment porewaters of the Santa Barbara Basin. *Geochim. Cosmochim. Acta.* **63,** 2199–2209.
Landing W. and Bruland K. (1987) The contrasting biogeochemistry of iron and manganese in the Pacific Ocean. *Geochim. Cosmochim. Acta.* **51(1),** 29–43.
Li Y.-H. and Gregory S. (1974) Diffusion of ions in sea water and in deep-sea sediments. *Geochim. Cosmochim. Acta.* **38,** 703–714.
Malcolm S. J. (1985) Early Diagenesis of Molybdenum in estuarine sediments. *Mar. Chem.* **16,** 213–225.
Moore W. S., Bruland K. W., and Michel J. (1981) Fluxes of uranium and thorium series isotopes in the Santa Barbara Basin. *Earth Planet. Sci. Lett.* **53,** 391–399.
Morford J. L. and Emerson S. (1999) The geochemistry of redox sensitive trace metals in sediments. *Geochim. Cosmochim. Acta.* **63,** 1735–1750.
Muramoto J. A., Honjo S., Fry B., Hay B. J., Howarth R. W., and Cisne J. L. (1991) Sulfur, iron and organic carbon fluxes in the Black Sea: sulfur isotopic evidence for origin of sulfur fluxes. *Deep-Sea Res.* **38 Suppl.2**, S1151–S1187.
Murray J. W., Jannasch H. W., Honjo S., Anderson R. F., Reeburgh W. S., Top A., Friederich G. E., Codispoti L. A., and Izdar E. (1989) Unexpected change in the oxic/anoxic interface in the Black Sea. *Nature.* **338,** 411–413.
NÆS K., Skei J. M., and Wassman P. (1988) Total particulate and organic fluxes in anoxic Framvaren waters. *Mar. Chem.* **23,** 257–268.
Nameroff T. J. (1996) Suboxic Trace Metal Geochemistry and Paleorecord in Continental Margin sediments of the Eastern Tropical North Pacific. Ph.D., University of Washington.
Pedersen T. F., Pickering M., Vogel J. S., Southon J. N., and Nelson D. E. (1988) The response of benthic foraminifera to productivity cycles in the eastern equatorial Pacific: Faunal and geochemical constraints on glacial bottom water oxygen level. *Paleoceanog.* **3,** 157–168.
Piper D. Z. and Isaacs C. M. (1996) Instability of bottom-water redox conditions during accumulation of Quaternary sediment in the Japan Sea. *Paleoceanog.* **11(2),** 171–190.
Platt T. H., W. G. (1985) Biogenic fluxes of carbon and oxygen in the ocean. *Nature.* **318,** 215–235.
Ravizza G., Turekian K. K., and Hay B. J. (1991) The geochemistry of rhenium and osmium in recent sediments from the Black Sea. *Geochim. Cosmochim. Acta.* **55,** 3741–3752.
Reimers C. E., Lange C. B., Tabak M., and Bernhard J. M. (1990) Seasonal spillover and varve formation in the Santa Barbara Basin, California. *Limnol. Oceanogr.* **35(7),** 1577–1585.
Reimers C. E., Ruttenberg K. C., Canfield D. E., Christiansen M. B., and Martin J. B. (1996) Porewater pH and authigenic phases formed in the uppermost sediments of the Santa Barbara Basin. *Geochim. Cosmochim. Acta.* **60(21),** 4037–4057.
Ricketts R. D. and Anderson R. F. (1998) A direct comparison between the historical record of lake level and the δ18O signal in carbonate sediments from Lake Turkana, Kenya. *Limnol. Oceanogr.* **43(5),** 811–822.
Schwalbach J. R. and Gorsline D. S. (1985) Holocene sediment budgets for the basins of the California Continental Borderland. *J. Sediment. Petrol.* **55,** 829–842.
Scranton M. I., Sayles F. L., Bacon M. P., and Brewer P. G. (1987) Temporal changes in the hydrography and chemistry of the Cariaco Trench. *Deep-Sea Res.* **34,** 945–963.M
Shaw T. J., Gieskes J. M., and Jahnke R. J. (1990) Early diagenesis in differing depositional environments: the response of transition metals in pore water. *Geochim. Cosmochim. Acta.* **54,** 1233–1246.
Shimmield G. B. and Price N. B. (1986) The behavior of molybdenum and manganese during early sediment diagenesis—offshore Baja California, Mexico. *Mar. Chem.* **19,** 261–280.
Sirocko F. (1995) Abrupt change in monsoonal climate: evidence from the geochemical composition of Arabian Sea sediments. Habilitation, University of Kiel.
Skei J. M., Loring D. H., and Rantala R. T. T. (1988) Partitioning and enrichment of trace metals in a sediment core from Framvaren, South Norway. *Mar. Chem.* **23,** 269–281.
Soutar A. (1971) Micropaleontology of anaerobic sediments and the California Current. In *The micropaleontology of oceans* (eds. B. M. Funnell and W. R. Ridell), pp. 223–230.
Taylor S. R. and McLennan S. M. (1985) The continental crust: its composition and evolution. Blackwells.
Thunell R. C., Tappa E., and Anderson D. M. (1995) Sediment fluxes and varve formation in Santa Barbara Basin. *Geology* **23(12),** 1083–1086.
Toole J., McKay K., and Baxter M. (1991) Determination of uranium in marine sediment pore waters by isotope dilution inductively coupled plasma mass spectrometry. *Analytica Chimica Acta.* **245,** 83–88.
Tucker M. D., Barton L. L., and Thomson B. M. (1997) Reduction and immobilization of molybdenum by Desulforvibrio desulfuricans. *J. Environ. Qual.* **26,** 1146–1152.
Wedepohl K. H. (1978) Molybdenum. In *Handbook of Geochemistry*, Vol. II (ed. K. H. Wedepohl). Springer-Verlag.
Williams R. J. P. (1994) The biogeochemistry of molybdenum. In *Molybdenum: An outline of its chemistry and uses* (eds. E. R. Braithwaite and J. Haber). Vol. 19, pp. 419–450. Elsevier.
Zheng Y. (1999) The marine geochemistry of germanium, molybdenum and uranium: the sinks. Ph.D., Columbia University.